REGIONAL MYOCARDIAL PERFUSION DATA WITH SPATIAL AND TEMPORAL QUANTIZATION

Ernest M. Stokely, L. R. Nardizzi, R. W. Parkey, and F. J. Bonte

Institute of Technology, Southern Methodist University, University of Texas Southwestern Medical School, and Parkland Memorial Hospital, Dallas, Texas

Regional ^{133}Xe washout data from normal and infarcted canine myocardia were collected using an Anger scintillation camera interfaced to a laboratory digital computer. Washout curves from selected regions were processed by a least-squares estimation program to determine the parameters of a three-compartment model. Various modifications in the methods of collection and generation of regional washout curves were then evaluated by examining the change in the slope of the first component of the model. The results suggest that to maintain an expected error of 10% or less, single-image data collection intervals of up to 10 sec and total-data collection (observation) times down to 1.5 min can be used. In severely infarcted hearts where inhomogeneous flows exist, washout curves from areas at the infarct boundary larger than 1 cm² tended to mask spatial flow patterns. An average error of 15.7% was detected when no compensation for nonmyocardial activity was performed on data from regions of infarction. Finally, the nonmyocardial background did not account for the tails (portion after 1.5 min) of washout curves from normal hearts.

Using radioactive xenon or krypton, several workers have investigated myocardial perfusion in humans and dogs (*1–11*). Little attention has been paid, however, to certain quantitative aspects of the myocardial perfusion curve. The growing use of Anger camera scintiphotography for assessment of myocardial perfusion in humans accentuates the need to optimize (A) the size of spatial areas of the cardiac images that are selected (spatial quantization of the image) for study of regional perfusion; (B) the length of the quantized time interval (data collection time) for generation of a single image; (C) the length of the total observation time over which data, or images, are collected; and (D) the effect of activity from the lung and other nonmyocardial structures on the myocardial perfusion curve should be evaluated.

It is important that the area of the spatial element and the length of the temporal collection interval be carefully chosen to minimize radiation exposure of the patient. Optimization occurs when the maximum spatial area and maximum time-collection interval are selected without significantly reducing the information content of the data that are collected during the removal of the isotope. Gamma-photon events can then be integrated over larger intervals of space and time, thereby reducing the required radionuclide dosage. Optimization of the temporal collection interval and the length of the observation time also means fewer images must be stored on the bulk storage device (magnetic-tape or magnetic-disk storage). Bulk storage costs are consequently minimized by eliminating the storage of unnecessary data.

The results presented here are derived using mongrel dogs as the experimental animal. Because of increased perfusion rates in the canine myocardium, the study of errors due to premature truncation of the washout curve does not directly apply to perfusion studies of the human heart. Other results, however, are pertinent to human myocardial perfusion studies, providing guidelines for selection of spatial and temporal quantization intervals and for correction of nonmyocardial background activity.

MATERIALS AND METHODS

Xenon-133 washout curves of the canine myocardium were generated in the following manner: Mongrel dogs weighing 15–25 kg were anesthetized

Received Sept. 14, 1972; revision accepted Mar. 25, 1973.

For reprints contact: Ernest M. Stokely, Dept. of Radiology, Parkland Memorial Hospital, 5323 Harry Hines Blvd., Dallas, Tex. 75235.

with intravenous sodium pentobarbital (30 mg/kg), strapped to a movable tabletop, and placed in the left lateral position. Through an incision of the left carotid artery, a 7F open-end catheter was inserted into the left anterior descending limb of the left coronary artery under fluoroscopic monitoring. The animal was then positioned over the Anger scintillation camera equipped with a magnifying collimator (*12*), having a useful resolution of approximately 1 cm. A 15–20 mCi bolus of ^{133}Xe dissolved in 2 ml of sterile saline was rapidly injected into the artery. The activity in the myocardium detected by the scintillation camera was collected over 3.5–4.0-sec intervals by a PDP-8/I computer system. The observation period began approximately 20 sec before injection and ended 5–18.5 min afterward, depending on the type of study. At the end of the data collection interval the entire digitized image from a 4,096-word section of computer memory was transcribed onto 7-track magnetic tape. By using the single-cycle data-break feature of the computer for collection of data, photon events for the next collection interval were stored in a different 4,096-word section of memory simultaneously as the image from the previous collection period was transcribed onto tape. This technique minimizes the overall computer-camera deadtime. The computer contains 12,288 words of memory and is interfaced to a graphics display terminal, a 262,144-word fixed-head magnetic disk, and a high-speed electrostatic line printer.

Myocardial ischemia was introduced by injecting 0.05 ml of mercury into the left coronary artery by a small catheter threaded inside the Number 7 catheter. The distribution of the mercury bolus in the myocardium was shown by radiographs. Xenon-133 was reinjected, and activity in the myocardium was again collected as previously described.

ANALYSIS METHODS

Images of xenon removal from the myocardium stored on 7-track magnetic tape were retrieved, read into the computer memory, and displayed on a storage oscilloscope. The area of the image to be investigated was selected, and a single washout curve was generated by summing points inside the selected area on subsequent images. The points of the resulting curve were then punched out onto paper tape for input to a Univac 1108 computer system where the curve was processed by BMDX85, a nonlinear least-squares program contained in the UCLA Biomedical Computer Program Package (*13*). This program allows the user to specify the form of an arbitrary mathematical function (model) which contains a number of unknown parameters. The values of these parameters are adjusted by the program so that the function optimally matches in a least-squares sense a data set supplied by the user. Starting values for the unknown parameters must be provided to the program.

The following multiexponential mathematical model was assumed to describe the curves,

$$\hat{y}(t) = C_1e^{-k_1t} + C_2e^{-k_2t} + \cdots C_me^{-k_mt} = \sum_{j=1}^{m} C_je^{-k_jt}. \quad (1)$$

The nonlinear least-squares program selected the value of each C and k in Eq. 1 so that the sum of the squared error [between $\hat{y}(t_i)$ and the ith data point] for all points on the washout curve was minimized. The curve-fitting procedure was repeated for a number of washout curves, using several different starting values for the unknown parameters. In every case the program converged to the same optimum values for C and k, showing an insensitivity to starting values and the presence of a global minimum.

The program allows the user to weight the error between $\hat{y}(t_i)$ and the data for each point in time. A set of weighting values was selected that provided a good fit of the model response to the washout curve (Fig. 1). For each curve approximately 60% of the initial portion of the error curve was given a weighting of 1.0, and the remaining 40% was given a weighting of 5.0. The effect of any estimation bias

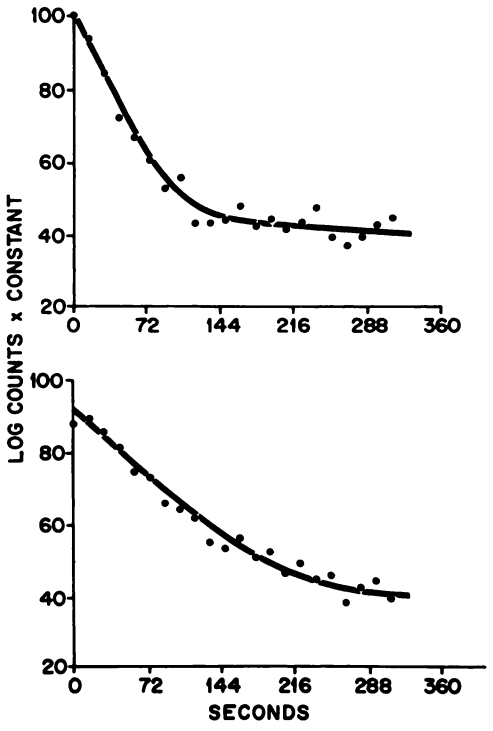

FIG. 1. Typical examples of washout curves and curves produced by model following curve-fitting procedure.

TABLE 1. ERRORS DUE TO TEMPORAL QUANTIZATION

Animal No.	Collection time: 3.6–4.0 sec k_1*	error (%)	7.2–8.0 sec k_1*	error (%)	14.4–16.0 sec k_1*	error (%)	24.0–25.2 sec k_1*	error (%)
111	−0.173	—	−0.176	1.27	−0.179	3.06	−0.182	4.79
112	−0.165	—	−0.174	5.08	−0.188	13.9	−0.206	24.4
113	−0.166	—	−0.170	2.23	−0.181	8.67	−0.191	15.1
114	−0.131	—	−0.132	0.46	−0.133	1.68	−0.129	−1.30
119	−0.142	—	−0.136	−4.22	−0.137	−1.35	−0.140	−3.86
128	−0.152	—	−0.150	−1.25	−0.151	−0.79	−0.153	1.06
Avg. error				0.60		4.20		6.70
s.d.				±2.88		±5.44		±10.8

* Values contain a scale factor dependent upon the collection interval.

is minimized by the subtraction operation in calculating the error, i.e.,

$$\% \text{ error} = \frac{k_1' - k_1}{k_1} 100\%, \qquad (2)$$

where k_1' is the value of k_1 after a modification of the data collection procedure.

Only the first three terms (m = 3) of Eq. 1 were used for modeling the washout curves. The nonlinear least-squares program was used to determine values for C_1, C_2, C_3, k_1, k_2, and k_3. The program often set C_3, k_2, or k_3 equal to zero.

Variations in the value of k_1 (Eq. 1) were computed for changes in collection interval, observation time, spatial area, and background correction. These variations are assumed to be homomorphically related to concurrent errors in the information content of the washout curve concerned with blood perfusion rate in the myocardium. This assumption is explored in more detail in the next section.

RESULTS AND DISCUSSION

Error due to extended time-collection intervals. The collection of myocardial images at data collection intervals of 3.6, 7.2, 14.4, and 25.2 sec was simulated by combining the counts in a selected area from n successive images to provide a single point on the washout curves.

$$n = \frac{\Delta_t'}{\Delta_t}, \qquad (3)$$

where n = number of images combined to provide a single point on the curve,

Δ_t' = simulated data collection interval in seconds, and

Δ_t = actual data collection interval in seconds used to record images.

The resulting washout curves were processed by the curve-fit program, and the values of k_1 obtained from the curves before and after the simulated change in the collection interval were compared. The error in k_1 due to the extended collection interval is presented in Table 1 and Fig. 2. For choosing the upper bound on the collection interval, it was arbitrarily assumed that a collection time should be selected so that the washout curves from at least 90% of the experimental animals could be expected to produce k_1 values having errors (due to the collection time) of less than 10%. A normal distribution was assumed for the data, and the 90 percentile locus was constructed as shown in Fig. 2. For example, to maintain errors of less than 10% (for 90% of the curves), a collection interval of 10 sec could be used.

Errors due to truncation of observation time. All

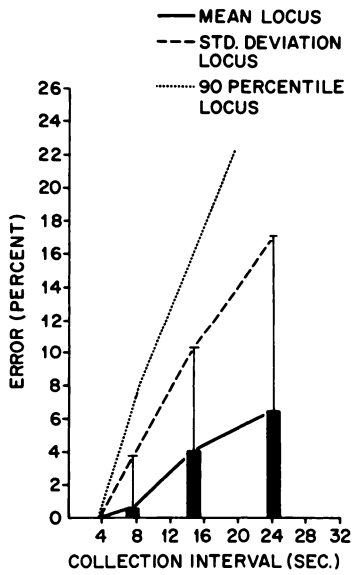

FIG. 2. Errors in calculated perfusion rates due to extended time intervals (sampling times) for forming each image.

TABLE 2. ERRORS DUE TO TRUNCATION OF OBSERVATION TIME

Animal No.	Observation time: 18.6 min k_1*	18.6 min error (%)	5.4 min k_1*	5.4 min error (%)	1.5 min k_1*	1.5 min error (%)	0.5 mni k_1*	0.5 mni error (%)
111	−0.169	—	−0.173	2.54	−0.170	0.30	−0.164	−2.90
112	−0.164	—	−0.165	1.04	−0.158	−3.42	−0.144	−12.0
113	−0.168	—	−0.166	−1.01	−0.161	−4.17	−0.133	−20.9
114	−0.133	—	−0.136	−1.51	−0.125	−5.51	−0.121	−8.82
119	—	—	−0.142	—	−0.144	1.55	−0.117	−17.7
128	—	—	−0.152	—	−0.149	−2.01	−0.132	−12.8
Avg. error				0.265		−3.20		−12.5
s.d.				±1.62*		±2.15		±5.82

* Values contain a scale factor dependent upon the collection interval.

slower time components of the model (Eq. 1) must be determined first if errors in the value of k_1 are tq be avoided. The "peeling" method (*14,15*) of curve-fitting a multiexponential model by hand is based on this effect. Computer programs such as those used here generate the solutions for all model parameters more or less simultaneously, but the effect of the slower time-constant terms on the value of k_1 are included in the solution. If the slower terms are incorrectly computed for whatever reason, the value of k_1 will be proportionately in error. In particular, if the slower components are not represented in the data due to premature truncation of the observation time, their effect on k_1 will not be accounted for, and errors in k_1 will result.

Xenon washout curves from six animals were used to investigate the error in k_1 due to truncation of the observation time. Four of the curves were carried out to 18.6 min. Using the value of k_1 for the 18.6-min observations, the errors of truncation at 5.6 min were computed. The total error was 0.265 ± 1.6%, a negligible amount. Truncation errors were also calculated for two additional curves that had been carried out to 5.4 min. The results are shown in Table 2 and the lower panel of Fig. 3.

In every case except Animal 128, the program found single-exponential models for the 0.5-min curves. For Animal 128, the error in k_1 using the curve-fitted values of a two-compartment model was +23.7%. When the model was constrained to a single exponential, the error in the value of k_1 was −12.8%, the value used in the error tabulation. This exception shows that care must be exercised when applying automatic curve-fitting techniques to severely truncated data. To test further the validity of the widespread practice of fitting the parameters of a single exponential model (m = 1, Eq. 1) to the initial segment of the washout curve, the six 1.5-min curves were reprocessed. The error in k_1 was −12.7 ± 9.9%.

Recalling that the curve-fitting program found single exponential models for all 0.5-min curves, the errors for a single compartment model fitted to data truncated to 0.5 and 1.5 min are 12.5 ± 5.8% and 12.7 ± 9.9%, respectively. Similar observation

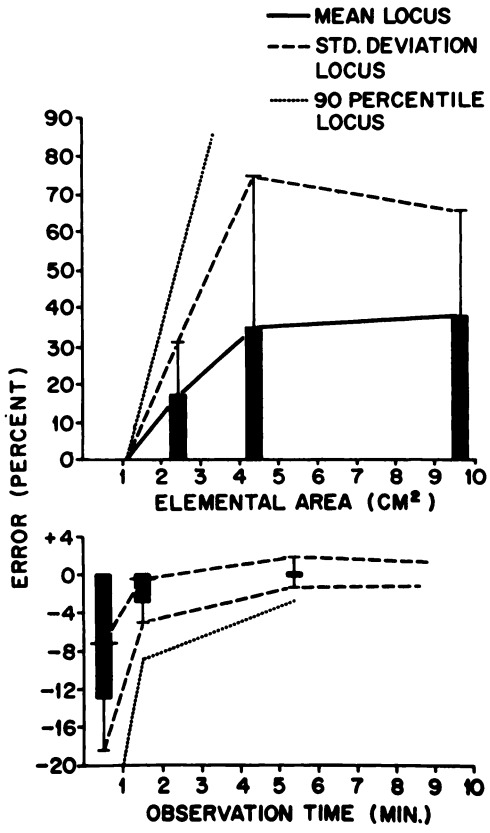

FIG. 3. Bottom panel shows errors in calculated perfusion rates due to premature truncation of total observation time (number of images collected). Errors in local perfusion rates due to investigation of flow over larger, encompassing areas of heart image are illustrated in top panel.

times are routinely used (*2,4,5*) to determine the slope of the washout curve for calculation of perfusion rates.

In the manner described in the section on the study of time quantization errors, a 90-percentile locus is included in Fig. 3. Using this locus and assuming that it is desirable to keep the errors due to observation time truncation below 10%, an observation time of at least 1.5 min is suggested (assuming the use of a multiexponential model).

Spatial quantization errors. In regional perfusion studies of the heart using an Anger camera, one or more elemental areas of the myocardial image are selected for investigation. Since all of the activity within a selected area is summed and reduced (quantized) to a single number for each image collected during isotope washout, any spatial flow gradients within the elemental area will be lost during the summation. Consequently, the size of the elemental area must be judiciously chosen to avoid serious degradation of the Anger camera's ability to resolve changes in the perfusion pattern that occur over small distances.

Regional myocardial perfusion is often studied by generating clearance curves from areas designated by a randomly oriented grid placed over the heart image. To test the effects of random-grid placement and grid size (spatial quantization), suppose the perfusion rate in the infarcted region is to be measured using such a grid system. A small area such as A4 (Fig. 4) can be placed within the infarcted region and a corresponding clearance curve can be generated. If successively larger areas are chosen to generate the clearance curve, the curve will eventually include unwanted activity from undamaged myocardium surrounding the infarction. This resulting perfusion error can be quantitatively measured for worst-case grid placement and grid size by choosing four self-encompassing areas as illustrated in Fig. 4. The largest area includes the infarct boundary where perfusion rates can be expected to be normal or supranormal (*16*). The experimental mercury embolus creates a worst-case, well-defined infarction supplied primarily by collateral pathways.

The k_1 value for area A4 is taken as the true (reference) value for perfusion rate within the infarction. This value is compared to k_1-values for areas A1, A2, and A3, and deviations are considered to be errors in the estimate of infarct perfusion due to grid size and grid placement.

The choice of test-area size was arbitrary in all cases except for the area A4, which was made as small as possible within certain constraints. A reasonable count level was maintained to avoid errors due to statistical data fluctuations that would interfere with the curve-fitting process. The average of the peaks of the washout curves generated from the area A4 (after subtraction of nonmyocardial activity) was 2,036 cpm providing reasonably good data for the curve-fitting program. In addition, the size of area A4 (1 cm^2) represents the limit of the usable resolution of the camera-collimator system with ^{133}Xe.

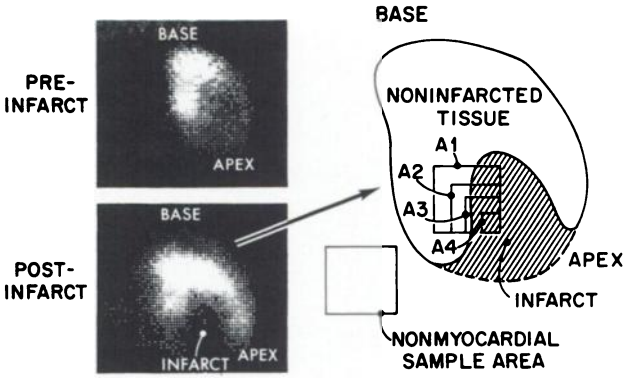

FIG. 4. Visualization of infarcted region is illustrated by oscilloscope photographs of heart image taken 5–10 sec after xenon injection. Sketch on right shows placement of areas for investigating loss of localized spatial flow information when larger areas of interest are chosen.

Table 3 summarizes the result of this study. The large error variation is due to variability in localization of the mercury embolus, the variations in placement of the elemental test areas, and variations in the physiological response. The upper panel of Fig. 3 is a plot of the error due to spatial quantization.

The large error value for Animal 108, area A2, apparently resulted from a large perfusion value for the tissue neighboring the infarct. Area A2 narrowly included the activity in this tissue whereas Areas 3 and 4 did not; hence, there was a large discrepancy in the error value. Area A1 contained the tissue with a high perfusion rate but also included a much larger area of the poorly perfused infarct.

Nonmyocardial background correction. As illustrated in Fig. 4, a nonmyocardial section of the washout adjacent to the myocardial test area was selected, and a nonmyocardial background curve was developed. The points on this curve were subtracted from points on the myocardial curve in the following manner:

$$z_i = \begin{cases} y_i - \dfrac{A_y}{A_x} x_i & \text{otherwise} \\ 0 \text{ for } \left(y_i - \dfrac{A_y}{A_x} x_i \right) < 0 & i = 1, 2, \cdots 1, \end{cases} \quad (4)$$

where z_i = new points of the curve corrected for background,

y_i = original points of myocardial curve,

TABLE 3. ERRORS DUE TO SPATIAL QUANTIZATION

No. Animal	Area 4 (1.1 cm²) k_1*	Area 3 (2.4 cm²) k_1*	Area 3 (2.4 cm²) error (%)	Area 2 (4.3 cm²) k_1*	Area 2 (4.3 cm²) error (%)	Area 1 (9.75 cm²) k_1*	Area 1 (9.75 cm²) error (%)
108	−0.207	−0.264	27.7	−0.425	106.0	−0.327	58.2
110	−0.206	−0.205	−0.50	−0.194	−5.90	−0.199	−3.70
119	−0.188	—	—	−0.194	3.10	−0.237	25.9
128	−0.113	−0.148	31.6	−0.146	29.8	−0.152	35.1
129	−0.043	−0.047	10.1	−0.062	44.1	−0.076	76.3
Avg. error			17.2		35.4		38.4
s.d.			±13.1		±39.6		±27.5

* Values contain a scale factor dependent upon the collection interval.

TABLE 4. ERRORS DUE TO NONMYOCARDIAL BACKGROUND ACTIVITY

Animal No.	Corrected for background k_1*	Not corrected for background k_1	Error (%)
105	−0.114	−0.091	−20.7
108	−0.339	−0.310	−8.64
109	−0.426	−0.370	−13.3
119	−0.203	−0.138	−31.9
128	−0.158	−0.152	−3.86
Avg. error			−15.7
s.d.			±9.83

* Values contain a scale factor dependent upon the collection interval.

x_l = points on nonmyocardial curve,

A_y = area of myocardium under investigation,

A_x = area of the nonmyocardial tissue, and

l = total number of points on curves.

The values of k_1 obtained by fitting the model parameters to y_l and z_l were compared, and the percent deviation was calculated.

Several areas from two normal hearts were processed in this manner. The effect of the nonmyocardial background was insignificant in every case. On the other hand, curves generated from severely infarcted regions were significantly modified by the background subtraction. Table 4 illustrates the results of this study for infarcted regions from five animals. One animal with an extremely localized mercury embolus exhibited a washout curve from the region of infarct that was totally canceled by the background subtraction, indicating essentially no blood perfusion of the infarct. Data from this area that had not been corrected for background would provide completely erroneous perfusion values.

These results suggest (A) that data from infarcted regions should be routinely corrected for nonmyocardial background activity before perfusion rates are computed, and (B) the tail of the washout curve from normal and most infarcted areas cannot be explained by the effect of nonmyocardial background activity alone.

Choice of k_1 as reference parameter. We have selected k_1 (Eq. 1), the value of the slope of the first component of the semilogarithmic multiexponential curve, as the parameter of the washout curve model that embodies the most information about blood perfusion in the myocardium. The sensitivity of this parameter to various methods of data collection and washout curve generation is used as an index to assess the loss from the washout curve of information relating to myocardial perfusion. Any error in k_1 is assumed to imply essentially the same error in the calculated perfusion rate, regardless of the mathematical model that is used.

The Kety-Schmidt (*17,18*) equation is usually used to calculate perfusion rate using the slope of a straight line that has been fitted from the first 40–90 sec of the semilogarithmic washout curve. This method is based on work by Cohen, et al (*4*), Herd, et al (*19*), Ross, et al (*2*), and Bassingthwaighte, et al (*20*), who showed that this technique provides a perfusion rate that is in good agreement with nitrous oxide perfusion rates or flow rates recorded during the metered infusion of blood into the coronary artery system. With the exception of the work of Bassingthwaighte, et al, it is not possible to determine from the results of the above investigations if trends exist in the deviation between the various methods of flow measurement.

Bassingthwaighte and his coworkers investigated several methods for determining the proper slope of the washout curve for use in the Kety-Schmidt equation. The so-called "flow-by-slope-at-30%-of-peak" method of determining the slope proved to be the most accurate. This technique determines the slope of a 38-sec period of the washout curve centered at a

time when the counting rate is 30% of the peak. Even though this technique provided the best average agreement to measured flows, their perfusion estimates exhibited an average error of −11% for all areas. By comparison, it has been shown here that a single-compartment curve fits to washout curves truncated to 0.5–1.5 min, which had a k_1 error of approximately −12.6%. These findings suggest that the value of k_1 from a multiexponential curve fit of the data of Bassingthwaighte, et al, (observed for 0.5–1.5 min) could be expected to yield converted perfusion values in very close agreement with the metered flow values. This would support the supposition that the parameter k_1 contains most of the information concerning perfusion rate.

SUMMARY

Regional ^{133}Xe washout data from normal and infarcted canine myocardia were analyzed to test the effects of various modifications in the method of data collection and washout curve generation. The effects of these modifications on the value of the slope of the first component of a multiexponential (up to three terms) model were studied.

Although the particular data presented here cannot be extrapolated directly to the human because of increased perfusion rates in the canine myocardium, the conclusions provide a conservative upper bound on the data collection period (10 sec for less than 10% error) and spatial size (1 cm^2) for human subjects. An observation time (total data collection interval) of 1.5 min was necessary to avoid data truncation errors of 10% or more although this finding does not apply to the collection of human data. The normal (noninfarcted) canine myocardium did not contain significant spatial perfusion gradients, but the infarcted canine heart was characterized by very inhomogeneous perfusion patterns. Finally, although nonmyocardial background activity was insignificant when compared with the activity in normal hearts, the washout curves from infarcted areas showed a 15.7 ± 9.8% error if not corrected for this effect. The tails (portion after 1.5 min) of washout curves from normal and most infarcted tissues were not explained by nonmyocardial background, nor were they explained by inhomogeneous spatial perfusion patterns. Others (*21*) have suggested that the departure of inert-gas washout curves from those of a single exponential model may be caused by arterial-to-venous shunting, counter-current exchange by capillaries, nonhomogeneous tissue structures, intercapillary diffusion gradients, xenon storage in epicardial fat, epicardial-endocardial perfusion rates, collateral flow or spatial perfusion patterns.

Correlation of the various types of errors that are tabulated here was not investigated, e.g., short observation times may increase the sensitivity to errors from increased data collection intervals. In addition, the significance of the various terms in Eq. 1 needed to describe the washout curves was not evaluated. These areas of investigation are suggested for future studies.

ACKNOWLEDGMENT

This work is supported by NIH Grants HL13625, HL05181, and NIH Training Grant CA05136. Ernest M. Stokely is an NIH Special Research Fellow (4FO3GM-42941). R. W. Parkey is a Scholar in Radiological Research, James Picker Foundation, NAS NRC.

REFERENCES

1. CANNON PJ, HAFT JI, JOHNSON PM: Visual assessment of regional myocardial perfusion utilizing radioactive xenon and scintillation photography. *Circulation* 40: 277–288, 1969

2. ROSS RS, UEDA K, LICHTLEN PR, et al: Measurement of myocardial blood flow in animals and man by selective injection of radioactive inert gas into the coronary arteries. *Cardiovasc Res* 15: 28–41, 1964

3. REES JR, REDDING VJ: Anastomotic blood flow in experimental myocardial infarction. *Cardiovasc Res* 1: 169–178, 1967

4. COHEN LS, ELLIOTT WC, GORLIN R: Measurement of myocardial blood flow using krypton 85. *Am J Physiol* 206: 997–999, 1964

5. HORWITZ LO, GORLIN R, TAYLOR WJ: Effects of nitroglycerine on regional myocardial blood flow in coronary artery disease. *J Clin Invest* 50: 1578, 1971

6. CHRISTENSEN EE, BONTE FJ: Radionuclide coronary angiography and myocardial blood flow. *Radiology* 95: 497–503, 1970

7. ANDERSEN H, BAGGER H, GOTZSCHE H: Non-uniform blood flow in the left ventricular wall of dogs measured by Xe-133 washout technique. *Acta Physiol Scand* 76: 376–382, 1969

8. REES JR, REDDING VJ, ASHFIELD R, et al: Myocardial blood flow measurement with 133 xenon-effect of glyceryl trinitrate in dogs. *Br Heart J* 28: 374–381, 1966

9. PARKEY RW, LEWIS SE, STOKELY EM, et al: Compartmental analysis of ^{133}Xenon regional myocardial blood flow curve. *Radiology* 104: 425, 1972

10. CANNON PJ, DELL RB, DWYER EM, Jr: Measurement of regional myocardial perfusion in man with ^{133}xenon and a scintillation camera. *J Clin Invest* 51: 964–977, 1972

11. CANNON PJ, DELL RB, DWYER EM: Regional myocardial perfusion rates in patients with coronary artery disease. *J Clin Invest* 51: 978–994, 1972

12. DOWDEY JE, BONTE FJ: Principles of scintillation camera image magnification with multichannel convergent collimators. *Radiology* 104: 89–96, 1972

13. DIXON WJ, ed: *Biomedical Programs—Supplement,* Berkeley, Univ of California Press, 1970

14. SHEPHERD CW: *Basic Principles of the Tracer Method.* New York, John Wiley & Sons, 1962, p 245

15. ATKINS GL: *Multicompartment Models for Biological Systems,* London, Methuen, 1969, p 101

16. REES JR, REDDING VJ: Experimental myocardial infarction in the dog. *Circ Res* 25: 161–170, 1969

17. KETY SS: Theory and applications of exchange of inert gas at the lungs and tissues. *Pharmacol Rev* 3: 1–41, 1951

18. KETY SS, SCHMIDT CF: Determination of cerebral blood flow in man by use of the nitrous oxide method. *Am J Physiol* 143: 53–66, 1945

19. HERD JA, HOLLENBERG M, THORBURN GD, et al: Myocardial blood flow determined with krypton 85 in unanesthetized dogs. *Am J Physiol* 203: 122–124, 1962

20. BASSINGTHWAIGHTE JB, STRANDELL T, DONALD DE: Estimation of coronary blood flow by washout of diffusible indicators. *Circ Res* 23: 259–278, 1968

21. SEJRSEN J: Convection and diffusion of inert gases in cutaneous, subcutaneous, and skeletal muscle tissue. In *Capillary Permeability,* Crone C, Lassen NA, eds, New York, Academic Press, 1970, pp 586–604